

# Filament seasoning and its effect on the chemistry prevailing in hot filament activated gas mixtures used in diamond chemical vapour deposition

Dane W. Comerford<sup>a</sup>, Ulrika F.S. D’Haenens-Johansson<sup>b</sup>, James A. Smith<sup>a</sup>,  
Michael N.R. Ashfold<sup>a,\*</sup>, Yuri A. Mankelevich<sup>c</sup>

<sup>a</sup> School of Chemistry, University of Bristol, Bristol, BS8 1TS, UK

<sup>b</sup> Department of Physics, University of Warwick, Coventry, CV4 7AL, UK

<sup>c</sup> Nuclear Physics Institute, Moscow State University, 119992 Moscow, Russia

Available online 18 June 2007

## Abstract

Tantalum hot filaments (HFs) find frequent use as a means of activating hydrocarbon/hydrogen mixtures used for chemical vapour deposition of thin film diamond. This contribution reports systematic studies of the power consumed by a tantalum HF, and companion laser based measurements of the relative H atom number densities in the gas phase adjacent to the HF surface, in pure H<sub>2</sub> and in dilute CH<sub>4</sub>/H<sub>2</sub> gas mixtures, as a function of process conditions (filament temperature, gas pressure, extent of HF carburisation). The measurements serve to highlight the way in which the adjacent gas phase chemistry and composition affects the HF surface chemistry, and vice versa.

© 2007 Elsevier B.V. All rights reserved.

**Keywords:** Diamond chemical vapour deposition; Hot filament; Hot-wire activation; H atoms; Gas phase laser diagnostics; Surface modification

## 1. Introduction

Hot filament (HF) activation of dilute hydrocarbon/H<sub>2</sub> (*e.g.* CH<sub>4</sub>/H<sub>2</sub>) gas mixtures is an established route for chemical vapour deposition (CVD) of thin film diamond [1–3]. Attractions of HF – compared with microwave or DC arc jet – activation include low cost, ease of implementation (making HF-CVD the method of choice for many small scale laboratory investigations) and its potential for scale-up to larger area deposition [4,5]. The technique has limitations also, principal amongst which are the limited purity of the as-grown diamond (which will almost inevitably be contaminated with trace quantities of the filament material) and the vulnerability of the HF to any oxygen in the source gas mixture. Despite its wide utility, however, there have been relatively few systematic studies of the HF itself, its evolution during an extended diamond deposition run, the way it responds to process conditions and the effect of such responses on the local gas phase chemistry it initiates.

The present work forms part of an on-going program, employing various laser diagnostics and complementary modelling, designed to explore the chemistry prevailing in HF activated H<sub>2</sub> [6], and CH<sub>4</sub>/H<sub>2</sub> [3,7–9] and B<sub>2</sub>H<sub>6</sub>/CH<sub>4</sub>/H<sub>2</sub> [10] gas mixtures used for CVD of undoped and B-doped diamond. Previous studies of HF activated H<sub>2</sub> and CH<sub>4</sub>/H<sub>2</sub> gas samples have identified much of the essential chemical physics: H atoms are formed by dissociative adsorption of H<sub>2</sub> at the HF surface, with an efficiency that increases rapidly with increasing filament temperature,  $T_{\text{fil}}$  [6,11,12]. These H atoms diffuse throughout the deposition chamber, and result in ratios of gas phase H atom to H<sub>2</sub> concentrations (henceforth represented as [H] and [H<sub>2</sub>]) in most parts of the reactor that are far in excess of that predicted on the basis of local thermodynamic equilibrium (reflecting the slow homogeneous recombination rate of H atoms at typical reactor pressures and temperatures) [2,3,6,13–17]. Laser probing studies (*e.g.* H atom Doppler lineshape measurements [6], and coherent anti-Stokes Raman spectroscopy measurements of H<sub>2</sub> rotational state population distributions [18]) have provided some of the most detailed gas temperature ( $T_{\text{gas}}$ ) profiles in HF reactors;  $T_{\text{gas}}$  near the HF ( $d < 1$  mm) is typically measured to be several 100 K lower than  $T_{\text{fil}}$  and thereafter to fall monotonically with increasing distance  $d$  from the HF [6,16,19,20]. Addition of

\* Corresponding author.

E-mail address: [mike.ashfold@bristol.ac.uk](mailto:mike.ashfold@bristol.ac.uk) (M.N.R. Ashfold).

hydrocarbon, or dopant (e.g. B<sub>2</sub>H<sub>6</sub>), introduces additional H atom loss mechanisms, initiating the series of ‘H-shifting’ reactions, radical formation and hydrocarbon cycling necessary for successful diamond CVD [2,3]. Quantifying the consequent reduction in [H] is complicated by possible additive induced changes to the HF, e.g. its resistivity and/or emissivity, and thus  $T_{\text{fil}}$  (and/or the power required to maintain any chosen  $T_{\text{fil}}$ ), and its ability to drive the dissociative adsorption of H<sub>2</sub>.

This contribution reports the results of systematic studies of the power consumed by a tantalum HF, and companion measurements of the local relative number densities of gas phase H atoms, in pure H<sub>2</sub> and in CH<sub>4</sub>/H<sub>2</sub> gas mixtures, which serve to illustrate further the complexity of the full range of chemical transformations involved in HF activated diamond CVD.

## 2. Experimental

The experimental apparatus and procedures have been described previously [6,10], and so only essential features are summarised here. The CVD chamber consists of a six-way cross, which can be evacuated to a base pressure of  $\sim 10^{-2}$  Torr by a two stage rotary pump connected to the lower arm. Three of the side-arms in the horizontal plane are fitted with quartz windows, two to allow exit and entrance of the laser radiation used for resonance enhanced multiphoton ionisation (REMPI) detection of H atoms while the third is an observation window that allows determination of  $T_{\text{fil}}$  using a two-color pyrometer (Land Infrared FRP12). All of the systematic studies reported here employed a Ta HF (250  $\mu\text{m}$  diameter, 7 turns with coil diameter  $\sim 3$  mm), mounted so that its long axis was parallel to the laser propagation axis. The accuracy of the  $T_{\text{fil}}$  value returned by the pyrometer was established by comparing the measured and literature (1769  $^{\circ}\text{C}$  [21]) temperature at which a Pt wire was melted by Joule heating. The pyrometer value was sensitive to the geometrical alignment but, when optimally aligned, was correct to within 50  $^{\circ}\text{C}$ . Under steady-state conditions the indicated temperature reading was stable to  $\pm 5$   $^{\circ}\text{C}$  in the range  $1800 < T_{\text{fil}} < 2500$   $^{\circ}\text{C}$ . H<sub>2</sub> and CH<sub>4</sub> flows were metered (in standard  $\text{cm}^3 \text{min}^{-1}$  (sccm)) using separate mass flow controllers (MFCs, Tylan), and pre-mixed in a manifold before introduction into the upper arm of the chamber, the total pressure in which was monitored using a 0–100 Torr capacitance manometer (Tylan Instruments). H atoms were detected by 2+1 REMPI on the  $2s \leftarrow 1s$  transition using 243.1 nm radiation generated by an Nd-YAG pumped dye laser (Continuum Surelite II plus Quanta-Ray PDL-3) operating at 10 Hz and subsequent frequency doubling (BBO crystal). Separation of the UV and fundamental dye laser radiation and normalisation of the measured REMPI signals for shot-to-shot variations in the intensity of the former was achieved as previously [6], while the frequency calibration and dispersion was monitored using a wavemeter (Coherent WaveMaster) and an etalon/photodiode combination. The UV radiation was focussed (20 cm focal length plano-convex lens) to a point  $d=1$  mm below the lower limb of the HF and the resulting H<sup>+</sup> ions collected on a negatively biased Pt probe wire as previously [6].

## 3. Results

The present data comprises measurements of power consumed,  $P$ , filament temperature,  $T_{\text{fil}}$ , and relative H atom number densities, [H], as a function of process conditions.

Fig. 1(a) shows power consumption data for bare Ta filaments maintained at three different  $T_{\text{fil}}$  values, 1800, 2000 and 2165  $^{\circ}\text{C}$ , as a function of H<sub>2</sub> pressure,  $p$ . The gas flow rate was maintained at  $F=100$  sccm throughout these measurements, and  $p$  varied by adjusting the throttling of the rotary pump. The general form of the measured  $P(p)$  profiles match those reported previously [22,23], and are each well described by a function of the form

$$P = P_{\text{rad}} + \frac{P_{\text{H}} K p}{1 + K p} \quad (1)$$

where  $K$  is a constant. Radiative heat transfer will dominate at the lowest pressures ( $p \sim 0$ ) [22,24]. The derived value for radiative power loss at these three temperatures,  $P_{\text{rad}}=18 \pm 1$ ,

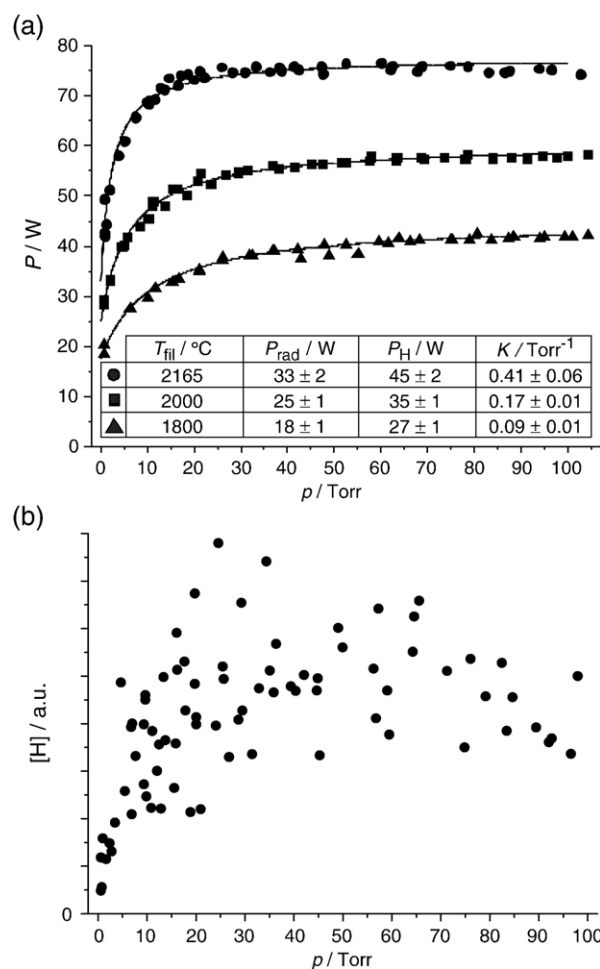


Fig. 1. (a) Electrical power,  $P$ , required to maintain Ta HFs at  $T_{\text{fil}}=1800$ , 2000 and 2165  $^{\circ}\text{C}$  at different H<sub>2</sub> pressures,  $p$ , and a total flow rate  $F=100$  sccm. The smooth curves through the data are best-fits obtained using Eq. (1) and the parameter values shown in the inset. (b) Relative H atom number density [H] measured as a function of  $p$  at  $d=1$  mm below the HF maintained at  $T_{\text{fil}}=2165$   $^{\circ}\text{C}$ .

25±1 and 33±2 W, are in sensible accord with that predicted using the Stefan–Boltzmann equation:

$$P_{\text{rad}} = \varepsilon \sigma T^4 S \quad (2)$$

with  $\varepsilon \sim 0.28$  [25] for Ta at  $T \sim 2165$  °C [26] and  $\sigma = 5.67 \times 10^{-12}$  W cm<sup>-2</sup> K<sup>-4</sup>. Setting  $P(p=0) = P_{\text{rad}}$  implies a value of  $S \sim 0.60$  cm<sup>2</sup> for the effective surface area for the emitting HF. Such is consistent with the observation that only the  $\sim 8$  cm coiled part of the HF attains white heat at  $T_{\text{fil}} = 2165$  °C if we introduce an additional geometric factor of 3/4 on the basis that  $\sim 1/2$  of the photons radiated from the interior surfaces of the coil are reabsorbed by the HF and thus do not contribute to  $P_{\text{rad}}$ . As Fig. 1(a) shows,  $P$  increases rapidly with  $p$  at low  $p$  but thereafter appears to saturate in a manner reminiscent of a Langmuir adsorption isotherm. Such a dependence supports the view that H atom production in such environments is by dissociative adsorption of H<sub>2</sub> on the HF surface [1–3], *i.e.*



where S\* represents an active site on the HF surface. We note, however, that use of an alternative form of Eq. (1) with  $(Kp)$  replaced by  $(Kp)^{1/2}$  (as would traditionally be used to describe a dissociative adsorption process) results in a poorer fit to the data, but returns broadly similar values for the pre-multiplier  $P_{\text{H}}$ . We rationalise this observation as follows: Given the effective bond dissociation energy  $D_0(\text{H–H}) = 456.7$  kJ mol<sup>-1</sup> at  $T \sim 2165$  °C [27] and the preceding estimate of  $S$ , the best-fit value of  $P_{\text{H}}$  at  $T \sim 2165$  °C (45±2 W) would imply an H atom production rate  $Q_{\text{H}} \sim 1.89 \times 10^{20}$  atoms cm<sup>-2</sup> s<sup>-1</sup>. This value is the upper limit, since the assumed  $P_{\text{H}}$  value includes heat conductive loss of power. Given that the (gas phase) equilibrium constant for the overall reaction



at 2165 °C is only  $\sim 0.02$  [27] and that our previous modelling of the gas phase chemistry prevailing at such  $T_{\text{fil}}$  values in this HF-CVD reactor [3,8,9] has required use of  $Q_{\text{H}}$  values at least 10× smaller than the upper limit value derived here, we deduce that only a small fraction of collisions of H<sub>2</sub> molecules with the filament surface contributes to  $Q_{\text{H}}$ . Most H<sub>2</sub>-surface collisions simply contribute to gas heating (either directly or through a balance of reactions (3) and (–3)). Such a view accords with previous conclusions regarding the variation of [H] – at constant  $p$  – with  $T_{\text{fil}}$  (and thus  $P$ ) [6,11], and with the present observation that [H], monitored by REMPI at 20 Torr H<sub>2</sub>, increases steeply in the ratio 1:~3:~7 as  $T_{\text{fil}}$  is increased from 1800, to 2000 and then 2165 °C.

Fig. 1(b) shows the variation of [H], measured at  $d=1$  mm, for the  $T_{\text{fil}}=2165$  °C case, plotted as a function of  $p$ . This profile also rises rapidly at low  $p$ , but has levelled off by  $p \sim 20$  Torr and declines gently at high  $p$ . Similar [H] versus  $p$  dependences have been reported previously [11,22,23] and, at the higher pressures, in our previous REMPI study [6]. All are consistent

with the view that H atom formation is mediated by adsorption onto the HF surface; the very gradual decline in [H] at higher  $p$  likely reflects an increasing contribution from gas phase three-body recombination of H atoms (the reverse of Eq. (5) with  $\text{M}=\text{H}_2$ ).

Curve (a) in Fig. 2 shows the variation of  $P$  with  $p$  for the case of a 1% CH<sub>4</sub> in H<sub>2</sub> gas mixture and a carburised Ta HF maintained at  $T_{\text{fil}}=2165$  °C. Carburisation was achieved by running a fresh Ta HF at this  $T_{\text{fil}}$  in 20 Torr of this gas mixture for  $\sim 10$  h prior to taking any measurements. The power required to maintain this  $T_{\text{fil}}$  at low  $p$  ( $P_{\text{rad}} \sim 57$  W) is higher than in the case of the bare Ta HF. This can be understood by attributing a higher emissivity ( $\varepsilon \sim 0.5$ ) to the carburised HF – consistent with the larger reported emissivities of tantalum carbides (*e.g.*  $\varepsilon(\text{TaC}) \sim 0.4$  [28]) and a carbonaceous layer such as might be found on the outer surface of a carburised HF (*e.g.*  $\varepsilon(\text{graphite}) \sim 0.95$ ). The power expended in activating adsorbed H<sub>2</sub>, in contrast, is less than in the case of a pure Ta HF. Analysis of data sets such as curve (a) in Fig. 2, yields average best-fit  $P_{\text{H}}$  values  $\sim 20$  W, validating previous reports that a carburised HF yields lower [H] than a bare metal HF maintained at the same  $T_{\text{fil}}$  [11]. Curve (b) in Fig. 2 shows the corresponding data obtained with the same carburised HF, but with a CH<sub>4</sub>-free gas flow. For these experiments, the 1% CH<sub>4</sub> contribution to  $F$  was switched off, and the HF was left to stabilise for a time  $t \sim 30$  min (during which  $P$  had to be raised progressively to maintain  $T_{\text{fil}}=2165$  °C) prior to taking measurements.  $P$  in this case rises more steeply with increasing  $p$ , maximising below 20 Torr. Curve (c) in Fig. 2 is the difference plot, obtained by comparing the  $(P-P_{\text{rad}})$  contributions in (a) and (b). The [H] versus  $p$  dependence for a 1% CH<sub>4</sub> in H<sub>2</sub> gas mixture and a carburised Ta HF (collected in tandem with the data shown in Fig. 2(a)) broadly parallels that measured in the

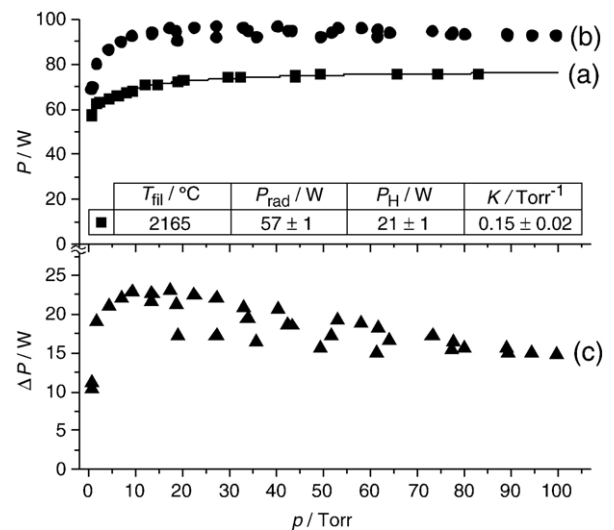


Fig. 2. Plots of  $P$  versus  $p$  for a carburised Ta HF maintained at  $T_{\text{fil}}=2165$  °C in the presence of (a) 1% CH<sub>4</sub> in H<sub>2</sub> and (b) H<sub>2</sub> at flow rates  $F=100$  sccm. The smooth curve in (a) is a best-fit to the data obtained using Eq. (1) and the parameter values shown in the inset. (c) Difference plot, obtained by comparing the  $(P-P_{\text{rad}})$  contributions in (a) and (b).

carbon free case (Fig. 1(b)), whereas the  $[H]$  versus  $p$  data recorded with  $H_2$  only and a carburised HF shows a more gradual increase with  $p$ , peaking at  $\sim 50$  Torr. Consideration of the relative magnitudes of  $[H]$  in the two cases is reserved until later.

Fig. 3 provides another visualisation of these process gas induced changes in  $P$ . Fig. 3(a) shows the variation in  $P$  over a continuous 16 h period, during which time  $F$ ,  $p$  and  $T_{\text{fil}}$  were maintained constant at 100 sccm, 20 Torr and 2165 °C, respectively. The experiment began with a virgin Ta HF, operating with pure  $H_2$ , throughout the period  $0 < t < 1$  h. The gas feed was switched to a 1%  $CH_4$  in  $H_2$  mixture and HF carburisation started at  $t = 1$  h. This flow was maintained until  $t \sim 8.75$  h.  $P$  changed little during this carburisation phase (although, as Figs. 1(a) and 2(a) show, the relative contribution

of  $P_{\text{rad}}$  must have changed considerably) and the HF resistance increased by  $\sim 30\%$ . The first discontinuity (at  $t \sim 8.75$  h) is the result of cutting off the  $CH_4$  component in  $F$ .  $P$  rises gradually, with a time constant  $\tau \sim 4$  min.  $P$  falls precipitously ( $\tau \ll 1$  min) when the 1%  $CH_4$  contribution to  $F$  is reinstated, but re-establishes its previous steady-state carburised value within  $\sim 5$  min. The later time part of the  $P$  versus  $t$  sequence shown in Fig. 3(a) displays the result of two further interruptions and re-establishments of the  $CH_4$  flow – demonstrating the reproducibility of the induced changes – and the longer term variation in  $P$  when the  $CH_4$  flow is stopped for good. Fig. 3(b) shows the  $P$  versus  $t$  variation during two  $CH_4$  interrupt/reinstate cycles on an expanded scale, along with the corresponding time dependent variation in  $[H]$ , for the case of  $p = 10$  Torr – chosen to highlight the sensitivity to process gas composition and HF carburisation (as revealed by curves (a) and (b) in Fig. 2). This shows an almost immediate doubling of  $[H]$  upon interrupting the  $CH_4$  flow, and a dramatic ( $> 80\%$ ) fall upon its reinstatement, followed by a more gradual recovery.

#### 4. Discussion

Ta HFs are used widely in diamond CVD. The carburisation rate of a Ta HF increases with increasing  $T_{\text{fil}}$ , % C in the process gas mixture and gas pressure, but is generally slower than for W, another commonly used HF material [24,29]. In both cases, carburisation involves dissolution of C at the HF surface, leading to the formation of an annular shell of sub-carbide ( $Ta_2C$  in this case) and carbide (TaC). Okoli et al. [29] have also proposed the presence of a thin carbonaceous surface layer on carburised Ta HFs operating under process conditions comparable to those used in the present work.

Such an HF structure would be consistent with the present observations that, apart from two  $P$  versus  $p$  plots in Fig. 1(a), were all made at constant  $T_{\text{fil}}$  (2165 °C). Under steady-state conditions, a carburised Ta HF operating with a 1%  $CH_4/H_2$  gas mixture yields a markedly lower local gas phase H atom number density than does a bare Ta HF operating in the same pressure of pure  $H_2$ . Indeed, Sommer and Smith [30] have reported that the  $H_2$  dissociation efficiency falls to near zero in the case that the HF is completely covered with graphite. Such observations encourage a picture of competitive adsorption: Ta lattice sites ‘blocked’ by adsorbed carbon atoms (or  $CH_x$  radicals) are not available to accommodate  $H_2$ , and the  $H_2$  dissociation rate (and thus the local  $[H]$ ) drops accordingly. Such a picture is also consistent with the observed increase in the fraction of  $P$  that is dissipated radiatively in the case of a carburised HF – reflecting the higher emissivities of carbide and carbonaceous surfaces.

The rapid changes in  $P$  and  $[H]$  upon interrupting and reinstating the 1%  $CH_4$  component to the total flow can be understood by recognising that any carbonaceous surface layer on a carburised HF is likely to be in a state of dynamic equilibrium. Growth of this layer will be by accommodation of gas phase carbon, thereby reducing  $Q_H$  and filament power losses. Possible loss processes from the carbonaceous coating would include dissolution into the bulk of the HF and reactive

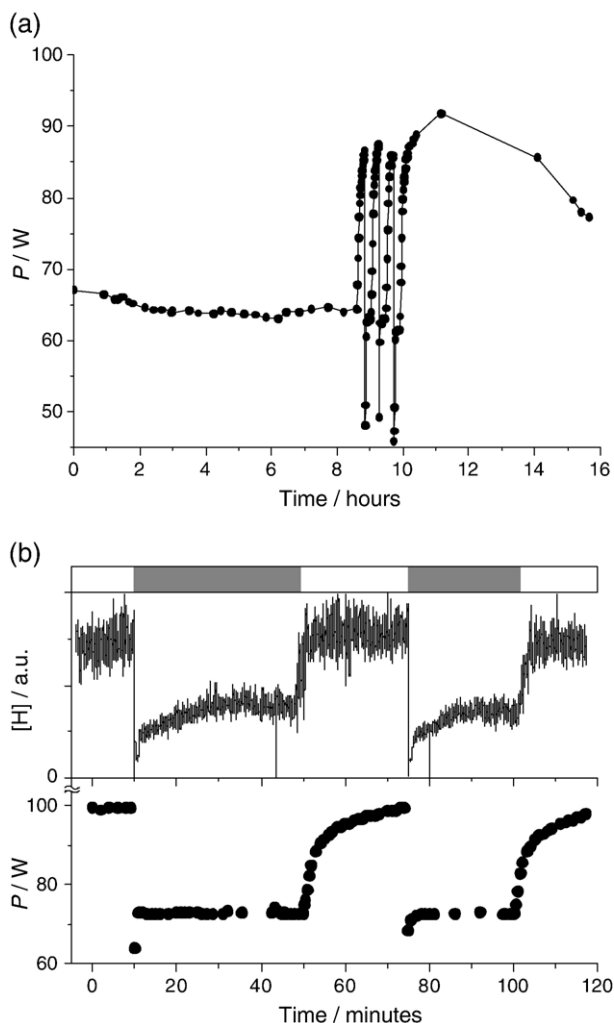
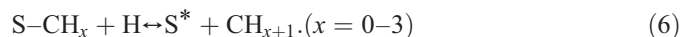


Fig. 3. (a) Plot of  $P$  versus  $t$  over a 16 h period during which the Ta HF was maintained at  $T_{\text{fil}} = 2165$  °C during carburisation with  $p = 20$  Torr of a 1%  $CH_4$  in  $H_2$  gas mixture ( $1 < t < 8.75$  h), subjected to three successive  $CH_4$  off/on cycles ( $8.75 < t < 10$  h) and then left to evolve for a further 6 h in a  $CH_4$ -free gas flow. (b) Expanded view of two  $CH_4$  off/on cycles together with the corresponding time dependent variation of  $[H]$ , both at  $p = 10$  Torr. The superimposed time bar indicates the presence (grey) or not (white) of the 1%  $CH_4$  component to the gas flow.

loss back into the gas phase. The latter process will involve variants of Eqs. (3) and (4), e.g.



Interrupting the CH<sub>4</sub> flow in the process gas mixture to a carburised HF will remove the carbon source for the external coating. It will also have the effect of switching off all gas phase ‘H-shifting’ reactions of the form C<sub>x</sub>H<sub>y</sub> + H ↔ C<sub>x</sub>H<sub>y-1</sub> + H<sub>2</sub>, thereby increasing [H], and thus the surface carbon removal rate. Thus we arrive at the following interpretation for the *P* and [H] versus *t* trends displayed in Fig. 3. Interrupting the CH<sub>4</sub> flow leads to progressive removal of the carbonaceous overcoat that is present on the carburised HF under steady-state conditions, exposing more of the underlying carbide. This surface modification leads to a gradual increase in *P*, over the timescale of several minutes; asymptotically, we observe an increase both in the power expended in gas activation (Fig. 2 (c)), and a modest increase in [H]. The timescale of minutes is determined by the time taken for removal of carbon species from the reactor volume as a result of diffusion and gas flow transfer processes [31]. Reinstating the CH<sub>4</sub> flow has an immediate and dramatic effect. *P* drops rapidly, consistent with *P*<sub>H</sub> falling as a result of efficient re-growth of the carbonaceous overcoat. As a result, [H] shows a similar sharp decline, reflecting the reduction in the number of surface sites at which it can accommodate and the sudden increase in gas phase loss processes.

This study suggests that deposition on, and loss processes from the HF surface are sufficiently fast that their respective rates will both depend on, and influence (through changes in *Q*<sub>H</sub>), the near filament gas phase species distributions. Such a conclusion is consistent with the fact that such a coating actually grows, and with the [total C<sub>x</sub>H<sub>y</sub>]/[H] gas phase number density ratio in the immediate vicinity of the HF. It also highlights the need for caution when attempting to rationalise any measured change in gas phase composition as a result of a change in process conditions simply in terms of gas phase chemistry. As we show here, relatively minor changes in process gas composition can also have a dramatic effect on the HF performance and function.

### Acknowledgements

We are grateful to EPSRC for the award of a portfolio grant (LASER), the Royal Society for a Joint Project Grant that enables the Bristol–Moscow collaboration, RFBR for Key Science Schools grant No. 7101.2006.2 (YuAM), and K.N.

Rosser for his many contributions to the experimental work described herein.

### References

- [1] F.G. Celii, J.E. Butler, *Ann. Rev. Phys. Chem.* 42 (1991) 643.
- [2] D.G. Goodwin, J.E. Butler, in: M.A. Prelas, G. Popovici, L.G. Bigelow (Eds.), *Handbook of Industrial Diamonds and Diamond Films*, Marcel Dekker, New York, 1998, p. 527.
- [3] M.N.R. Ashfold, P.W. May, J.R. Petherbridge, K.N. Rosser, J.A. Smith, Yu.A. Mankelevich, N.V. Suetin, *Phys. Chem. Chem. Phys.* 3 (2001) 3471.
- [4] See, for example, <http://www.seki.com.sg/sp3.html>.
- [5] J. Zimmer, K.V. Ravi, *Diam. Rel. Mater.* 15 (2006) 229.
- [6] S.A. Redman, C. Chung, K.N. Rosser, M.N.R. Ashfold, *Phys. Chem. Chem. Phys.* 1 (1999) 1415.
- [7] J.A. Smith, E. Cameron, M.N.R. Ashfold, Yu.A. Mankelevich, N.V. Suetin, *Diam. Rel. Mater.* 10 (2001) 358.
- [8] Yu.A. Mankelevich, N.V. Suetin, M.N.R. Ashfold, J.A. Smith, E. Cameron, *Diam. Rel. Mater.* 10 (2001) 364.
- [9] J.A. Smith, J.B. Wills, H.S. Moores, A.J. Orr-Ewing, M.N.R. Ashfold, Yu. A. Mankelevich, N.V. Suetin, *J. Appl. Phys.* 92 (2002) 672.
- [10] D.W. Comerford, A. Cheesman, T.P.F. Carpenter, D.M.E. Davies, N.A. Fox, R.S. Sage, J.A. Smith, M.N.R. Ashfold, Yu.A. Mankelevich, *J. Phys. Chem. A* 110 (2006) 2868.
- [11] F.G. Celii, J.E. Butler, *Appl. Phys. Lett.* 54 (1989) 1031.
- [12] D.M. Li, R. Hernberg, T. Mäntylä, *Diam. Rel. Mater.* 7 (1998) 1709.
- [13] L. Schafer, C.-P. Klages, U. Meier, K. Kohse-Hoinghaus, *Appl. Phys. Lett.* 58 (1991) 571.
- [14] M. Chenevier, J.C. Cubertafon, A. Campargue, J.P. Booth, *Diam. Rel. Mater.* 3 (1994) 587.
- [15] K.-H. Chen, M.-C. Chuang, C.M. Penney, W.F. Banholzer, *J. Appl. Phys.* 71 (1992) 1485.
- [16] L.L. Connell, J.W. Fleming, H.-N. Chu, D.J. Vestek Jr., E. Jensen, J.E. Butler, *J. Appl. Phys.* 78 (1995) 3622.
- [17] V. Zumbach, J. Schafer, J. Tobai, M. Ridder, T. Dreier, B. Ruf, F. Behrendt, O. Deutschmann, J. Warnatz, *J. Chem. Phys.* 107 (1997) 5918.
- [18] S.O. Hay, W.C. Roman, M.B. Colket III, *J. Mater. Res.* 5 (1990) 2387.
- [19] U. Meier, K. Kohse-Hoinghaus, L. Schafer, C.-P. Klages, *Appl. Opt.* 29 (1990) 4993.
- [20] M.A. Childs, K.L. Menningen, L.W. Anderson, J.E. Lawler, *J. Chem. Phys.* 104 (1996) 9111.
- [21] J. Emsley, *The Elements*, 2nd edn. Clarendon Press, Oxford, 1989.
- [22] T. Otsuka, M. Ihara, H. Komiyama, *J. Appl. Phys.* 77 (1995) 893.
- [23] S. Schwarz, S.M. Rosiwal, M. Frank, D. Breidt, R.F. Singer, *Diam. Rel. Mater.* 11 (2002) 589.
- [24] E. Zeiler, S. Schwarz, S.M. Rosiwal, R.F. Singer, *Mater. Sci. Eng. A335* (2002) 236.
- [25] Y.S. Touloukian, D.P. DeWitt (Eds.), *Thermophysical Properties of Matter: Thermal Radiative Properties*, IFI/Plenum, New York, 1970, p. 654.
- [26] R.D. Allen, L.F. Glasier, P.L. Jordan, *J. Appl. Phys.* 31 (1960) 1382.
- [27] M.W. Chase Jr., *J. Phys. Chem. Ref. Data*, Monograph 9 (1998).
- [28] B.H. Eckstein, R. Forman, *J. Appl. Phys.* 33 (1962) 82.
- [29] S. Okoli, R. Haubner, B. Lux, *Surf. Coat. Technol.* 47 (1991) 585.
- [30] M. Sommer, F.W. Smith, *J. Mater. Res.* 5 (1990) 2433.
- [31] J.B. Wills, M.N.R. Ashfold, A.J. Orr-Ewing, Yu.A. Mankelevich, N.V. Suetin, *Diam. Rel. Mater.* 12 (2003) 1346.